Benha Journal of Applied Sciences (BJAS) **print: ISSN 2356–9751**
Vol. (10) Issue (2) (2025), (1-8) **online: ISSN 2356–976x**

http://bjas.bu.edu.eg

Applied and Basic Science

Antimicrobial activity of Cichorium intybus leaves extracts

Hoda F.Elbadawy[1] , Mervat G.Hassan[1] , Dina M.Baraka[1], Hamed M.Elshora[2] and Gharieb S.El-Sayyad[3]

[1]Botany and Microbiology, Dept., Faculty of Science, Benha Univ., Benha, Egypt
[2]Botany Dept., Faculty of Science,Mansoura University,Mansoura,Dakahlia, Egypt.
[3]Drug Radiation Research Dept., National Center for Radiation Research and Technology (NCRRT), Egyptian Atomic Energy Authority (EAEA), Cairo, Egypt

E-mail: hoda.ghoniem@fsc.bu.edu.eg

Abstract

Plants have formed the foundation of traditional medicine for hundreds of years, and they still provide humanity with novel answers. The phrase "medical plant" has been defined in the literature as the direct application of different plant parts or the active compounds produced from them in the treatment of illnesses. Because they are a source of therapeutic phytochemicals that will enable the creation of new medications, medicinal plants are extremely important. *Cichorium intybus* extracts (water and ethanolic) were assayed for the evaluation of their antimicrobial activity against four bacterial strains: *Escherichia coli, Listeria monocytogenes, Pseudomonas aeruginosa, and Staphylococcus aureus* , two fungal *Aspergillus niger* and *Fusarium exosporium* and *C. albicans*

Key Words: Aspergillus niger, C. albicans, Cichorium intybus, Escherichia coli, Fusarium exosporium, Listeria monocytogenes, Pseudomonas aeruginosa, Staphylococcus aureus.

1.Introduction

The Asteraceae family includes the two-year-old chicory (Cichorium intybus L.), which has comparatively flat leaves and a pile root system. The plant's name is a combination of Greek and Latin. The plant is commonly known as *chicory* due to its distinctive flower bed, and the scientific name *Cichorium intybus* is derived from this characteristic.

The genus Cichorium may thrive in nearly every type of soil. Coffee is made with chicory roots. The plant's body and leaves are used to make vegetable meals and salads.

Both alcoholic and non-alcoholic drinks contain chicory extracts. The public uses various portions of chicory as a diuretic, pain reliever, and laxative.

[2]. Chicory is regarded as a medicinal plant, and its root, stem, and flower all contain compounds that have antiviral, anticancer, and antidiabetic properties. [4].

Phytochemical analyses of chicory have identified a range of active compounds, including inulin, flavonoids, alkaloids, volatile compounds, oils, terpenes, coumarins, hydroxycoumarins, proteins, vitamins, polynes, and sesquiterpene lactones such as lactusin, lactucopyrrin, 8-desoxy lactusin, and guaianolid glycosidase. These compounds contribute to the plant's medicinal properties and potential therapeutic applications.

In addition to all of these compounds, the plant may have a variety of pharmacological effects, including sedative, wound healing, anticancer, hepatoprotective, hypolipidemic, cardiovascular, antioxidant, antidiabetic, and gastroprotective effects [1]. According to other related studies, chicory ethanol extracts have antioxidant effect since they can stop peroxide from forming in prime steam lard [11]. Chicory water extracts have demonstrated a strong antioxidant impact on LDL, as well as inhibitory effects on the breakdown of fatty acids in LDL and the generation of thiobarbituric acid reactive compounds [10]

2.Materials and Methods

Plant material :-

The fresh leaves of *Cichorium intybus* were harvested in 2023 from Mansoura. Upon arrival at the laboratory, the samples were carefully examined to remove any soil particles and unhealthy portions. The leaves were then air-dried in a shaded environment at room temperature until they reached a constant weight. Afterward, they were finely ground into a powder and stored for various analyses.

Selective Extraction Technique :-

The air-dried powdered leaves of the plant were subjected to a comprehensive extraction process using a Soxhlet apparatus. The extraction was carried out in two phases, first using water and then with 70% ethanol as solvents to ensure complete extraction of the active compounds from the plant material, allowing for the thorough isolation of bioactive constituents present in both aqueous and ethanol extracts.

To measure the antimicrobial activity of water and ethanolic extracts of *Portulaca oleracea* against the four bacterial strain *Escherichia coli, Listeria monocytogenes, Pseudomonas aeruginosa, and Staphylococcus aureus* , two

fungal *Aspergillus niger* and *Fusarium exosporium* and *C. albicans* were used as test organisms [3]. The antimicrobial activity of the test extracts was assessed using 96-well flat polystyrene plates. Initially, 10 µl of the test extracts were introduced into each well, achieving a final concentration of 250 µg/ml. To this, 80 µl of lysogeny broth (LB broth) was added, followed by 10 µl of microbial culture suspension during its log phase. The plates were then incubated overnight at 37°C to allow for bacterial growth and interaction with the extracts. After the incubation period, the antimicrobial effect of the tested compounds was assessed based on the clearance observed in the wells. A clear zone indicated that the extract had an inhibitory effect on the bacterial growth, whereas wells containing no active compound appeared opaque due to the continued bacterial growth. For comparison, a control with the pathogen without treatment was also included. Absorbance measurements were taken approximately 20 hours post-incubation at OD600 using a Spectrostar Nano Microplate Reader (BMG LABTECH GmbH, Allmendgrun, Germany), to quantify bacterial growth inhibition.

In a parallel experiment, the synthesis and characterization of Bimetallic MgO-ZnO nanoparticles (NPs) were also conducted.

The absorbance and spectral properties of the synthesized bimetallic MgO-ZnO nanoparticles (NPs) were thoroughly analyzed using a UV-Vis spectrophotometer (JASCO V-560). To ensure accuracy, an additional experiment was conducted without any metal ions for Auto-zero calibration. Initially, the optical characteristics of each sample were studied to identify the range of wavelengths necessary to effectively assess the absorbance properties of the NPs. To further understand the particle characteristics, the size distribution of the bimetallic MgO-ZnO NPs was measured using dynamic light scattering (DLS) analysis. This was performed at the St. Barbara facility in California, USA, utilizing the DLS-PSS-NICOMP 380-ZLS particle-sizing system. A small cuvette containing 100 µL of the bimetallic MgO-ZnO NP suspension was prepared for analysis. The system was allowed to reach equilibrium for two minutes at a temperature of 25.0 ± 2°C, and five separate measurements were performed to ensure the consistency and reliability of the results.

The mean size distribution of the synthesized bimetallic MgO-ZnO NPs was determined using DLS measurements conducted at the St. Barbara facility in California, USA, employing the DLS-PSS-NICOMP 380-ZLS particle-sizing system. For the analysis, a small cuvette containing 100 µL of the bimetallic MgO-ZnO NP suspension was used temporarily to carry out the measurements.

After reaching equilibrium for two minutes at an ambient temperature of 25.0 ± 2°C, five separate measurements were performed.

To further characterize the synthesized bimetallic MgO-ZnO NPs, HR-TEM (JEM2100, Jeol, Japan) was employed to analyze their size, shape, and overall morphology. Additionally, crystallization properties, crystallite diameters, and morphology were examined using XRD (Shimadzu XRD-6000), with the 2θ diffraction angle used to assess X-ray power.

The bimetallic MgO-ZnO NPs, stabilized by the water extract of *Cichorium intybus* leaves, were also analyzed using SEM (ZEISS EVO-MA10, Germany) to evaluate their surface structure and arrangement. Furthermore, surface charges of the synthesized NPs were measured using a Zeta potential analyzer from Malvern Devices, UK, at the preparation pH [22].

3.Results

Bioassay against bacteria and fungi

Antibacterial activity

The presented data outlines the antimicrobial efficacy of different compounds water extract of *Cichorium intybus* (B1) and 70 ٪ethanolic extract of *Cichorium intybus* (B2) against four bacterial strains: Escherichia coli, Listeria monocytogenes, Pseudomonas aeruginosa, and Staphylococcus aureus. The antibacterial activity was quantified in terms of percentage inhibition, where higher values indicate greater efficacy.

For water extract of *Cichorium intybus* (B1) Escherichia coli exhibited a moderate inhibition of 23.15% In the case of Listeria monocytogenes, water extract of *Cichorium intybus* (B1) demonstrated substantial inhibition, Against Pseudomonas aeruginosa, Ethanolic extract of *Cichorium intybus* (B2) displayed the highest activity among all compounds, with an inhibition of In the case of Staphylococcus aureus, water extract of *Cichorium intybus* (B1) exhibited moderate inhibition (23.00%)Moving on to70 ٪ethanolic extract of *Cichorium intybus (* B2) displayed improved antibacterial activity compared to their B1 counterparts across all tested strains

Table(1) :Antibacterial activity of water and ethanolic extracts of *Cichorium intybus*:-

Sample	Antibacterial activity (%) *Staphylococcu*	*Pseudomonas*	*Listeria*	*Escherichia*

	s aureus	*auruginose*	*monocytogenes*	*coli*
(water extract of *Cichorium intybus*) B1	23.00000	9.24824	45.02200	23.15350
(70 ٪ethanolic extract of *Cichorium intybus*) B2	46.00000	35.55976	21.00000	23.01030
Ciprofloxacin	98.00223	99.23651	97.93214	98.36987

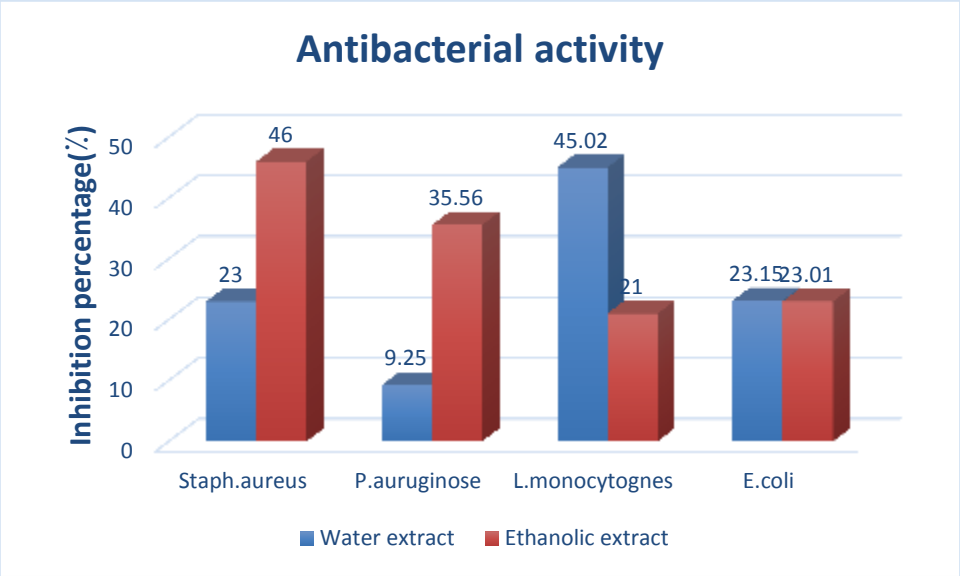

Fig.(1) Antibacterial activity of water and ethanolic extracts of *Cichorium intybus*:-

ANTIFUNGAL activity:-

The provided data illustrates the antimicrobial activity of different compounds water extract of *Cichorium intybus* (B1),and 70 ٪ethanolic extract of *Cichorium intybus (* B2), against two fungal strains: *Aspergillus niger* and *Fusarium exosporium*

The values in the table represent the percentage of inhibition or activity against each fungal strain. Ethanolic extract of *Cichorium intybus* (B2) shows no activity against *Aspergillus niger and C. albicans* but exhibits significant inhibition (64.19%) against *Fusarium exosporium*. 70 water extract of *Cichorium intybus* (B1) show high activity against *Aspergillus niger(80.86)* and shows moderate inhibition (40.23%) against *C. albicans*.

Table(2) :Antifungal activity of water and ethanolic extracts of *Cichorium intybus*:-

Sample	Antifungal activity (%)		
	F. exosporium	*A .niger*	*C. albicans*
(water extract of *Cichorium intybus*) B1	80.86460348	3.773584906	40.23.773584
(70 ٪ethanolic extract of *Cichorium intybus*) B2	64.18762089	0	0
Nystatin (10ug/ml)	98.12531255	99.33662534	98.42241130

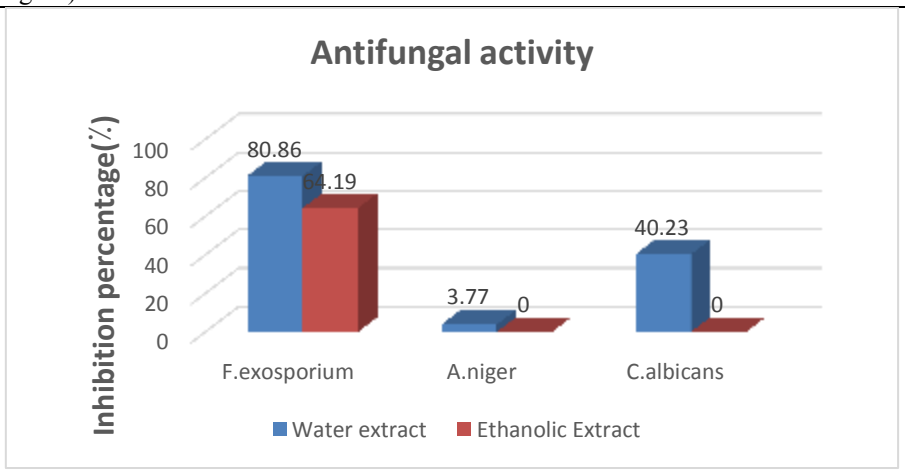

Fig.(2) Antifungal activity of water and ethanolic extracts of *Cichorium intybus*:-

Synthesis and characterization of bimetallic MgO-ZnO NPs

The optical absorbance and spectral characteristics of the synthesized bimetallic MgO-ZnO nanoparticles (NPs) were systematically analyzed using UV-Vis spectroscopy. A characteristic absorbance peak was observed at an optical density (OD) of 1.2, corresponding to a visible absorption at 400 nm. The absorption spectrum exhibited a broad peak, spanning wavelengths from 270 nm to 500 nm. This broad absorption range can be attributed to several factors including the poly-dispersed nature of the synthesized NPs, variations in particle size distribution, the polydispersity index (PDI), and surface defects, which were confirmed by complementary characterization techniques such as dynamic light scattering (DLS), scanning electron microscopy (SEM), and high-resolution transmission electron microscopy (HR-TEM). Additionally, the bimetallic interaction between MgO and ZnO contributes significantly to the observed spectral properties, which is consistent with the typical behavior of metal oxide nanoparticles**.**

The particle size distribution and dispersion characteristics of the synthesized bimetallic MgO-ZnO NPs were determined using DLS. This analysis provided detailed information on the hydrodynamic diameter, size distribution, and degree of polydispersity. The HR-TEM images revealed that the nanoparticles were predominantly semi-spherical in shape, with sizes ranging from 22.78 nm to 89.34 nm, and an average size of 33.45 ± 1.5 nm. This size distribution reflects the reduction mechanism facilitated by the water extract of Cichorium intybus leaves, which acted as a stabilizing agent, likely reducing the size of the nanoparticles and controlling their shape. The radical-mediated reduction process facilitated by the extract is believed to have led to the formation of nanoparticles with varying sizes, which was consistent with the findings from previous studies in the literature**.**

Upon comparing the synthesized bimetallic MgO-ZnO NPs with previous reports, it was evident that the particles exhibited poly-dispersity, with a dominant spherical morphology. This variability in particle size and morphology may be attributed to the use of Cichorium intybus leaf extract as a capping and reducing agent, which could introduce variability in nanoparticle formation. The DLS analysis showed that the average size of the nanoparticles was approximately 80.34 nm, which is considered to be within the range of acceptable size for nanoparticles in biological applications. According to the International Standards Organization (ISO), samples with a PDI value above 0.05 are classified as polydisperse, and the PDI value of 0.91 obtained in this study corroborates this classification**.**

HR-TEM analysis further confirmed the spherical shape of the synthesized nanoparticles, with a slightly smaller average particle size compared to that measured by DLS. The difference in size estimation between the two techniques can be attributed to the difference in measurement principles, with DLS providing a hydrodynamic diameter of the particles in solution, while HR-TEM images reveal the actual size of individual particles. The Zeta potential of the MgO-ZnO NPs was measured at a pH of 7.1, and a negative value of -40.44 mV was observed. This negative surface charge is likely due to the presence of negatively charged functional groups from the Cichorium intybus leaf extract, which contributes to the stability of the nanoparticles by preventing aggregation through electrostatic repulsion**.**

To further investigate the surface morphology and structural integrity of the synthesized nanoparticles, SEM was employed. The SEM images showed that the surface of the MgO-ZnO NPs was smooth and well-defined, with spherical particles being the predominant morphology. The Cichorium intybus leaf extract facilitated the formation of these uniform spherical particles, which were clearly illuminated under SEM, suggesting effective stabilization and capping of the nanoparticles. The presence of the plant extract was crucial in controlling the size and shape of the nanoparticles, and it appeared to play a key role in partitioning the MgO-ZnO NPs into well-defined spherical structures**.**

X-ray diffraction (XRD) analysis was performed to assess the crystallinity and phase structure of the synthesized bimetallic MgO-ZnO NPs. The XRD patterns exhibited both amorphous and crystalline phases in the nanocomposite, with distinct diffraction peaks corresponding to the crystalline phases of ZnO and MgO. The diffraction peaks observed at 2θ values of 27.50°, 47.15°, 56.80°, 66.58°, and 71.25° correspond to Bragg's reflections (002), (101), (102), (110), (103), and (201), respectively, and are consistent with the face-centered cubic (fcc) crystal structure of ZnO. These peaks align with the standard JCPDS card number 36-1451, confirming the crystalline nature of the MgO-ZnO NPs. The XRD results conclusively demonstrated the successful synthesis of highly crystalline

MgO-ZnO NPs with a well-defined fcc crystal structure, further supporting the synthesis and structural integrity of the bimetallic nanoparticles.

4.Disscussion:-

Bioassay against bacteria and fungi

The antibacterial properties of an organic acid-rich extract from fresh red chicory (*Cichorium intybus* var. sylvestre) were examined against periodontopathic bacteria, including *Streptococcus mutans*, *Actinomyces naeslundii*, and *Prevotella intermedia*. The active extract was found to contain several bioactive compounds, such as shikimic acid, quinic acid, succinic acid, and oxalic acid, which are believed to contribute to its antimicrobial activity.

With varying degrees of effectiveness, it was shown that all organic acids reduced the development of biofilms and the adherence of bacteria to cells. These substances also caused the cultured substratum and shikimic acid to break down biofilms and separate dead cells.

[5]. In additional research on the antimicrobial properties of *Cichorium intybus*, it was found that both crude aqueous and organic seed extracts exhibited significant activity against a range of pathogenic microorganisms. These included *Salmonella typhi*, *Bacillus subtilis*, *Staphylococcus aureus*, *Micrococcus luteus*, and *Escherichia coli*. Furthermore, root extracts, rich in vitamins and polynes, were notably effective in inhibiting the growth of these pathogens. [6, 7].

Additionally, a modest level of efficacy against multidrug-resistant S. typhi was demonstrated by the leaf extract of C. intybus [8]. C. intybus root preparations high in guaianolides have demonstrated antifungal activity against anthropophilic fungus. Salmonella typhi, Micrococcus luteus, E. coli, Trichophyton tonsurans, Trichophyton rubrum, and Trichophyton violaceum aureus vitamins, polynes

[7].Strong antifungal action against Pseudomonas cichorii was demonstrated by cichoralexin, a sesquiterpenoid phytoalexin that was extracted from chicory [9].

Chicory extracts have demonstrated the ability to inhibit the growth of several pathogenic microorganisms, including *Sarcina lutea*, *Agrobacterium tumefaciens*, *Erwinia carotovora*, *Pseudomonas aeruginosa*, *Pseudomonas fluorescens*, as well as both zoophilic and anthropophilic dermatophytes [12,13].

Furthermore, Petrovic's research revealed that root extracts exhibit stronger antibacterial activity compared to extracts derived from the whole plant [12].

In terms of bacterial susceptibility, Gram-positive bacteria, with the notable exception of *Bacillus subtilis*, were generally more responsive to chicory extracts than their Gram-negative counterparts. This differential susceptibility can be attributed to the hydrophilic cell wall structure of Gram-negative bacteria, which is largely composed of lipopolysaccharides (LPS). The presence of LPS impedes the accumulation of phenolic compounds within the target bacterial membrane, making Gram-negative bacteria more resistant to the antimicrobial effects of chicory extracts [14].

The majority of bioactive substances, including polyphenolics (such flavonoids and tannins), are found in solvents with a higher polarity. Significant antibacterial activity levels were demonstrated by the 70% ethanol and acetic ether extracts, which had higher TPC values, against the majority of the bacterium under study. The polyphenols, tannins, and coumarins included in crude extracts are responsible for this antibacterial action [16; 15; 17].

By altering their permeability, phenolic chemicals may target cell walls and membranes, allowing intracellular components to be released and disrupting membrane function (Bajpai and colleagues 2009).

Chicory possesses a number of sesquiterpene lactones, particularly in the roots [21,19].

Eight α-angeloyloxycichoralexin, a novel antimicrobial sesquiterpenoid discovered by Nishimura, has antifungal properties. Additionally, they have separated and identified two types of guaianolides (cichoralexin and 10 α-hydroxycichopumilide) in accordance with a chicory defense mechanism that has been postulated. Furthermore, they have found that adding dry chicory rhizome powder to food prolongs its shelf life and that ether-soluble phenolics from the rhizome contain nematoidal properties [20].

Synthesis and characterization of bimetallic MgO-ZnO NPs

The UV-Vis spectra of the initial precursors, zinc acetate and magnesium acetate, displayed distinct absorption peaks at different wavelengths: zinc acetate exhibited a peak at 290 nm [23], while magnesium acetate showed its absorption at 230 nm [24]

The intensity of the brown hue correlated with the ability for biosynthesis bimetallic MgO-ZnO NPs that was generated [25-27]. Surface Plasmon Resonance (SPR) is notably influenced by various factors, including the intensity, size, morphology, and dielectric properties of the nanoparticles produced

[29,28]**.** By correlating the experimental data with HR-TEM results, we determined the average size of the produced NPs [30]. The water extract of *C. intybus* leaves, rich in active functional groups, played a pivotal role in stabilizing and reducing the concentration of these groups, acting as capping agents to form polydispersed NPs [31]**.** Mohsin and colleagues [37] synthesized bimetallic Ag-Au core-shell NPs by adjusting the pH and temperature during the citrate reduction process. These parameters were crucial for determining particle morphology and size, with specifications that particles should be spheroidal and range from 50 to 65 nm. The HR-TEM images showed uniform line spacing, indicating a single-grade system, with Mg uniformly distributed in the Zn matrix, forming a unique alloy [32]**.** The polydispersed NPs in this study offer a long-term solution, thanks to the use of *C. intybus* leaf extract as a reducing and capping agent [33]. polydispersity index (PDI) values less than 0.05 indicate a uniform particle distribution, while values above 0.7 suggest a variable distribution [34]. The synthesized nanocomposite demonstrated a satisfactory polymorphism range, as indicated by the findings in the present study [35].

According to citation [36], several key factors contribute to the significant size of the nanocomposite, including its internal hydrodynamic radius and the water layers that surround it. The hydrodynamic radius is crucial in determining the overall dimensions of the nanoparticles, influencing both their size distribution and interaction with the surrounding environment.

The surrounding water layers also play a vital role in stabilizing the particles, potentially affecting their dispersion in a solution. It is noteworthy that the 2θ values correspond to the water extract of *Cichorium intybus* leaves, with a 2θ range extending from 5° to 21° [32]. In reference to the standard JCPDS card number 36-1451, specific diffraction peaks at 2θ values of 27.40°, 31.22°, 45.54°, 56.56°, 67.17°, and 75.56° are observed. These diffraction peaks correspond to Bragg's reflections at the following angles: (002), (101), (102), (110), (103), and (201), respectively [38].

XRD data provided valuable insights into the interaction between the bimetallic nanoparticles and the amorphous water extract of *Cichorium intybus* leaves. The data confirmed the structural integrity of the nanoparticles and contributed significantly to improving their dispersion in solution. The well-dispersed nanoparticles are crucial for enhancing their stability and effectiveness, thus broadening their potential applications in various fields, such as nanomedicine, catalysis, and environmental remediation [40]**.**

Additionally, the crystallite size of the bimetallic MgO-ZnO NPs was accurately determined using the Williamson-Hall (W H) equation [41, 42].This method, which is based on the analysis of X-ray diffraction peak broadening, yielded a crystallite size of 22.34 nm.

5.Conclusion

This study details the antibacterial properties of Cichorium intybus water and ethanolic extract.Cichorium intybus extracts were shown to be abundant sources of important components and phytochemicals with a wide range of therapeutic uses when the microbiological qualities of specific medicinal plant extracts were evaluated against bacteria and fungi. Both are regarded as effective substitutes for antibiotics in the management of bacterial and fungal infections.

Reference

[1] AE, Al-Snafi. Medical importance of *Cichorium intybus* – A review. *IOSR Journal Pharmacy*, .2016; vol, 6,pp: 41-56.

[2] HP, Bais & GA, Ravishankar. *Cichorium intybus* L. cultivation, processing, utility, value addition and biotechnology, with an emphasis on current status and future prospects *J. Sci. Food Agric*;2001.vol,81, pp: 467-484

[3] HA, Alhadrami AM, Hassan R, Chinnappan H, Al-Hadrami WH, Abdulaal EI, Azhar et al. Peptide substrate screening for the diagnosis of SARS-CoV-2 using fluorescence resonance energy transfer (FRET) assay. *Microchimica Acta*; 2021,vol, *188*, pp:1-10.

[4] RA, Street J, Sidana & G, Prinsloo. *Cichorium intybus*: traditional uses, phytochemistry, pharmacology, and toxicology. *Evidence- Based Complementary and Alternative Medicine*, 2013.

[5] G, Gazzani M, Daglia A, Papetti and C, Gregotti. "*In vitro* and *ex vivo* anti- and prooxidant components of *Cichorium intybus*," *Journal of Pharmaceutical and Biomedical Analysis*; 2000,vol. 23, no. 1, pp. 127–133.

[6] T, Shaikh RA, Rub and S, Sasikumar. "Antimicrobial screening of *Cichorium intybus* seed extracts," *Arabian Journal of Chemistry*, 2012.

[7] D, Mares C, Romagnoli B, Tosi E, Andreotti G, Chillemi and F, Poli.

"Chicory extracts from *Cichorium intybus* L. as potential antifungals," *Mycopathologia*; 2005, vol. 160, no. 1, pp. 85–91.

[8] P, Rani and N, Khullar. "Antimicrobial evaluation of some medicinal plants for their anti-enteric potential against multi-drug resistant *Salmonella typhi*," *Phytotherapy Research*; 2004, vol. 18, no. 8, pp. 670–673.

[9] K, Monde T, Oya A, Shirata and M, Takasugi. "A guaianolide phytoalexin, cichoralexin, from *Cichorium intybus*," *Phytochemistry*; 1990, vol. 29, no. 11, pp. 3449–3451.

[10] TW, Kim KS, Yang. Antioxidative effects of Cichorium intybus root extract on LDL (low density lipoprotein) oxidation. Arch Pharmacal Res ; 2001. Vol, 24(5):pp: 431–6.

[11] S, Riaz Tanzeel-ur-Rehman, IU, Khan MZ, Qurashi P, John M, Hassan R, Kausar et al. Comparison of antioxidant activity of *Cichorium intybus* by using different reported antioxidant assays. Asian J Chem; 2011,vol, 23(5):pp: 2201–6.

[12] J, Petrovic A, Stanojkovic L, Comic S, Curcic. Antibacterial activity of *Cichorium intybus*. Fitoterapia ;2004, Vol,75(7–8):pp: 737–9.

[13] D, Mares C, Romagnoli B, Tosi E, Andreotti G, Chillemi F, Poli. Chicory extracts from Cichorium intybus L. as potential antifungals. Mycopathologia ;2005, vol, 160(1):pp: 85–92.

[14] N, Bezic M, Skocibusic V, Dunkic A, Radonic. Composition and antimicrobial activity of *Achillea clavennae* L. essential oil. Phytother Res ;2003,vol,17(9):pp:1037–40.

[15] T, Allahghadri I, Rasooli P, Owlia MJ, Nadooshan T, Ghazanfari M, Taghizadeh et al. Antimicrobial property, antioxidant capacity, and cytotoxicity of essential oil from cumin produced in Iran. J Food Sci ;2010,vol, 75(2):pp: H54–61.

[16] S, Kilani M, Ben I, Sghaier I, Limem J, Bouhlel W, Boubaker et al. In vitro evaluation of antibacterial, antioxidant, cytotoxic and apoptotic activities of the tubers infusion and extracts of Cyperus rotundus. Bioresource Technol ;2008, vol, 99(18):pp: 9004–8

[17] JF, Ayala-Zavala C, Rosas-Dominguez V, Vega-Vega GA, Gonzalez-Aguilar. Antioxidant enrichment and antimicrobial protection of fresh-cut fruits using their own byproducts: looking for integral exploitation. J Food Sci ;2010, vol, 75(8):pp:R175–81.

[18] VK, Bajpai SM, Al-Reza UK, Choi JH, Lee SC, Kang. Chemical composition, antibacterial and antioxidant activities of leaf essential oil and extracts of Metasequioa glyptostroboides Miki ex Hu. Food Chem Toxicol ;2009,vol,47(8):pp:1876–83.

[19] F, Poli G, Sacchetti B, Tosi M, Fogagnolo G, Chillemi R, Lazzarin et al. Variation in the content of the main guaianolides and sugars in *Cichorium intybus* var. "Rosso di Chioggia" selections during cultivation. Food Chem ;2002,vol, 76(2):pp:139–47.

[20] H, Nishimura Y, Kondo T, Nagasaka A, Satoh. Allelochemicals in chicory and utilization in processed foods. J Chemical Ecol ;2000, vol,26(9):pp:2233–41

[21] AM, Peters A, van Amerongen. Sesquiterpene lactones in chicory (*Cichorium intybus* L) – Distribution in chicons and effect of storage. Food Res Intl ;1996, vol, 29(5–6):pp: 439–44.

[22] A, Said et al. Antibacterial activity of green synthesized silver nanoparticles using lawsonia inermis against common pathogens from urinary tract infection. Applied Biochemistry and Biotechnology, 2023: pp: 1-14**.**

[23] AA, Barzinjy and HH, Azeez. Green synthesis and characterization of zinc oxide nanoparticles using Eucalyptus globulus Labill. leaf extract and zinc nitrate hexahydrate salt. SN Applied Sciences; 2020, Vol, 2(5): pp: 991**.**

[24] H, Rani et al. In-vitro catalytic, antimicrobial and antioxidant activities of bioengineered copper quantum dots using Mangifera indica (L.) leaf extract. Materials Chemistry and Physics, 2020. vol, 239: pp: 122052**.**

[25] A, Fouda et al. Optimization of green biosynthesized visible light active CuO/ZnO nano-photocatalysts for the degradation of organic methylene blue dye. Heliyon, 2020. vol, 6(9): pp: e04896**.**

[26] R, Munir et al. Biosynthesis of Leucaena Leucocephala leaf mediated ZnO, CuO, MnO2, and MgO based nano-adsorbents for Reactive Golden Yellow-145 (RY-145) and Direct Red-31 (DR-31) dye removal from textile wastewater to reuse in agricultural purpose. Separation and Purification Technology, 2023. Vol,306: pp: 122527**.**

[27] AA, Badawy et al. Efficacy assessment of biosynthesized copper oxide nanoparticles

(cuo-nps) on stored grain insects and their impacts on morphological and physiological traits of wheat (triticum aestivum l.) plant. Biology;2021, vol, 10(3): pp: 233.

[28] KL, Kelly et al. The optical properties of metal nanoparticles: the influence of size, shape, and dielectric environment. 2003, ACS Publications.

[29] KS, Prasad and K, Selvaraj. Biogenic synthesis of selenium nanoparticles and their effect on As (III)-induced toxicity on human lymphocytes. Biological trace element research, 2014. vol,157(3): pp: 275-283.

[30] A, Lawrie et al. Microparticle sizing by dynamic light scattering in fresh-frozen plasma. Vox sanguinis, 2009. vol, 96(3): pp: 206-212.

[31] P, Monika et al. Recent advances in pomegranate peel extract mediated nanoparticles for clinical and biomedical applications. Biotechnology and Genetic Engineering Reviews, 2022: pp:1-29.

[32] AI, El-Batal et al. Gum Arabic polymer-stabilized and Gamma rays-assisted synthesis of bimetallic silver-gold nanoparticles: Powerful antimicrobial and antibiofilm activities against pathogenic microbes isolated from diabetic foot patients. International Journal of Biological Macromolecules, 2020. vol,165: pp: 169-186.

[33] E, Castro-Longoria AR, Vilchis-Nestor, and M, Avalos-Borja. Biosynthesis of silver, gold and bimetallic nanoparticles using the filamentous fungus Neurospora crassa. Colloids and Surfaces B: Biointerfaces, 2011. vol,83(1): pp: 42-48.

[34] M, Nissen et al. Nanoparticle Tracking in Single-Antiresonant-Element Fiber for High-Precision Size Distribution Analysis of Mono-and Polydisperse Samples. Small, 2022. vol,18(38): pp: 2202024.

[35] SS, Salem. Bio-fabrication of selenium nanoparticles using Baker's yeast extract and its antimicrobial efficacy on food borne pathogens. Applied Biochemistry and Biotechnology, 2022. vol,194(5): pp: 1898-1910.

[36] TG, Souza VS, Ciminelli and NDS, Mohallem. A comparison of TEM and DLS methods to characterize size distribution of ceramic nanoparticles. in Journal of Physics: Conference Series. 2016. IOP Publishing.

[37] M, Mohsin et al. An Insight into the Coating Behavior of Bimetallic Silver and Gold Core-Shell Nanoparticles. PLASMONICS, 2020.

[38] F, Bigdeli and A, Morsali. Synthesis ZnO nanoparticles from a new Zinc (II) coordination polymer precursor. Materials Letters, 2010. vol,64(1): pp: 4-5.

[39] MA, Siddiquee et al. Biogenic synthesis, in-vitro cytotoxicity, esterase activity and interaction studies of copper oxide nanoparticles with lysozyme. Journal of Materials Research and Technology, 2021. vol,13: pp: 2066-2077.

[40] S, Poyraz et al. One-step synthesis and characterization of polyaniline nanofiber/silver nanoparticle composite networks as antibacterial agents. Acs Applied Materials & Interfaces, 2014. vol, 6(22): pp: 20025-20034.

[41] P, Belavi et al. Structural, electrical and magnetic properties of cadmium substituted nickel–copper ferrites. Materials Chemistry and Physics, 2012. vol, 132(1): pp: 138-144.

[42] K, Pal MA, Elkodous, and MM, Mohan. CdS nanowires encapsulated liquid crystal in-plane switching of LCD device. Journal of Materials Science: Materials in Electronics, 2018. vol, 29(12): pp: 10301-10310.